

OPTIMIZATION OF SEMI-SOLID HIGH-PRESSURE DIE CASTING PROCESS BY COMPUTER SIMULATION, TAGUCHI METHOD AND GREY RELATIONAL ANALYSIS

Ivana Dumanić , Sonja Jozić, Dražen Bajić, and Jure Krolo

Faculty of Electrical Engineering, Mechanical Engineering and Naval Architecture, University of Split, Ruđera Boškovića 32, 21000 Split, Croatia

Copyright © 2020 American Foundry Society
<https://doi.org/10.1007/s40962-020-00422-5>

Abstract

The main aim of this research was to simulate high-pressure die casting of A356 semi-solid aluminum alloy using casting process simulation tool. Taking into account the viscosity of the semi-solid slurry and the mold-filling characteristics in high-pressure die casting, the mold for semi-solid aluminum alloy had been designed. Also, the influence of the three input parameters (liquid fraction of slurry, plunger velocity at 2nd phase and mold geometry) on the casting time, shrinkage and bubble formation during semi-solid high-pressure die casting processes were investigated. The Taguchi-based 'grey relational analysis' approach was used to identify the optimal process

parameters. A method used in this study for finding out the importance of the controllable parameter on the performance characteristic is called the analysis of variance. It was observed that the optimal parameters are the liquid fraction of 50%, the plunger velocity at 2nd phase of 1 m/s and the angle between the vertical plane and the cavity of 60°.

Keywords: semi-solid, high-pressure die casting, simulation, aluminum alloy, Taguchi design, grey relational analysis

Introduction

Semi-solid metal (SSM) processing is a technique which involves the formation of metal alloys between the solidus temperature and the liquidus temperature. These alloys consist of a liquid phase and a solid phase. Thus, these alloys are called semi-solid slurry. In the 1970s, it was discovered that metallic alloys in the semi-solid state with specific (globular) microstructure could display thixotropy.¹ Because of the thixotropy, physical basics of semi-solid slurry can be explained as follows: When the slurry is at rest, gravity will bring the particles into contact and the semi-solid material will support its own weight. Also, during a deformation, shear breaks the bonds, and viscous flow of the material occurs.² In other words, when the semi-solid slurry flows into the mold, under the influence of a shear force, its viscosity decreases. It is able to fill the cavity in a laminar manner.³ The fluid which surrounds solid globules acts as a lubricant, and hence, a higher fluidity and lower viscosity are obtained.²

Because SSM processing is an intermediate technique, it has advantages compared with conventional forging and conventional casting manufacturing techniques. Some advantages are follows: limited risk of gas entrapment and low shrinkage porosity due to laminar flow,⁴ energy efficiency,⁵ prolonged mold life due to less thermal shock,⁶ good dimensional tolerances,³ reduced defects and entrained oxides,⁷ etc.

Based on the above-mentioned, it can be concluded that achieving thixotropic properties of slurries, i.e., production of nondendritic, globular, and microstructure, is the key point of semi-solid metal forming processes. There are two main groups of SSM technologies: rheo-routes and thixo-routes. The rheo-routes refer to the preparation of an SSM slurry with a solid globular microstructure directly from a liquid phase and its injection into a die or a mold (e.g., rheo-high pressure die casting R-HPDC,⁸ ultrasonic treatment,⁹ electromagnetic stirring,^{10,11} superheat casting,¹² new rheocasting semi-solid metal processing technology NRC,¹³ etc.). The thixo-routes refer to a process in which preparation of a thixo-feedstock material with the globular

microstructure, its reheating in the semi-solid range and its shaping are involved (e.g., thixomolding,¹⁴ thermomechanical treatments,¹⁵ spray casting,¹⁶ etc.).

High pressure die casting (HPDC) is a technique in which products are formed by forcing molten metal into a mold or a die at high pressure and relatively high speed. Good surface finish, accurate dimension and mass production are some of the advantages of HPDC process.¹⁷⁻¹⁹ However, to increase quality, SSM has been added to the process. R-HPDC, NRC and gas-induced semi-solid (GISS) are some of the rheo-routes that have been adapted to high-pressure die casting for eliminating its disadvantages (solidification shrinkage and porosity resulting from gas entrapment^{20,21}).

On the other hand, in semi-solid HPDC process, it is essential to optimize parameters which may influence the quality of process. Fluidity, solidification and thus the mechanical properties are, among other things, affected by temperature of the slurry, temperature of mold, plunger velocity (injection speed, the metal velocity at the gate) and process pressure.

Nourouzi et al.²² investigated the optimal metal forming process parameters (in the semi-solid cooling slope method) of semi-solid A356 alloy. The aim was to get the minimum grain size by optimizing cooling coefficient parameters, pouring temperature and die cavity temperature. For optimization, they applied a genetic algorithm (GA). Khosravi et al.²³ investigated the optimal cooling coefficient parameters and pouring parameters at the same semi-solid process in order to determinate the maximum globularity of A356 alloy. They adopted the D-optimal experimental design of experiment. Using Taguchi optimization methodology, Suslu et al.²⁴ minimized porosity in GISS-HPDC process and EN-AC 48000 aluminum alloy. Controllable parameters were melt temperature, gas blowing time, 2nd phase velocity and gate thickness.

Moreover, numerical simulations of semi-solid process based on HPDC have been used to save time, to reduce the cost required to design a casting system and to identify positional problems during filling. Numerical simulations give the opportunity to produce high-quality product without performing numerous experimentation.

As noted earlier, casting geometry and velocity parameters have influence on formation of different phenomena during semi-solid die casting (e.g., microporosity, turbulent flow and unfilled phenomena). Therefore, to prevent these phenomena, optimization of the casting process parameters (liquid fraction of the slurry and plunger velocity at 2nd phase) and mold geometry is presented in this paper. The Taguchi design approach is adopted for experimental planning. Also, grey relational analysis is used to find optimal casting process parameters for multi-objective

function. To reduce the time and cost in mold design, all experiments were performed in virtual environment using a commercial software code, NovaFlow&Solid. Therefore, in the next sections by the term 'experiment' is meant simulation of the process. This special program designed for casting simulations is based on the control volume mesh technology and enables the very fast and reliable precise generation of the results. No need for empirical tests, less material waste and improved quality are also some of the benefits of usage of this software.

Theory and Material

Description of Solidification Calculation Theory

The commercial software used in this study, NovaFlow&Solid, is based on control volume mesh technology (CVM). This finite volume method allows the surface of the 3D model to control the shape of the mesh elements on the border of the casting.²⁵ The software's model of alloy crystallization is based on the macroscopic theory of quasi-equilibrium two-phase zone. Due to the fact that alloys crystallize in the range between solidus and liquidus temperatures, liquid phase and solid phase are present. Two-phase zone theory assumes that sum of volumetric fraction of the solid phase, $S(t)$, volumetric fraction of the liquid phase, $L(t)$, and volumetric fraction of the emptiness, $P(t)$, is equal to one²⁵:

$$S(t) + L(t) + P(t) = 1 \quad \text{Eqn. 1}$$

where t is time.

Mathematically, phase balance in time derivation from zero to one takes a form:

$$\frac{\partial S(t)}{\partial t} + \frac{\partial L(t)}{\partial t} + \frac{\partial P(t)}{\partial t} = 0 \quad \text{Eqn. 2}$$

Reduced law of mass conservation is:

$$\rho_s(T) \frac{\partial S}{\partial t} + \frac{\partial}{\partial t} (\rho_L(T)L) = 0 \quad \text{Eqn. 3}$$

where $\rho_s(T)$ and $\rho_L(T)$ are densities of the liquid phase and solid phase of the metal as temperature functions, respectively.

Reduced law of mass conservation for alloy components is:

$$\rho_s(T) C_S^i(T) \frac{\partial S}{\partial t} + \frac{\partial}{\partial t} (C_L^i(T) \rho_L(T)L) = 0 \quad \text{Eqn. 4}$$

where $C_S^i(T)$ and $C_L^i(T)$ are concentrations of the i -th alloy component solid phase and the liquid phase, respectively, at temperature T . These concentrations are defined from the phase constitutional diagram of the multi-component system.

The heat conduction with sources and convective heat transfer is given by the equation:

$$\begin{aligned}
 & S\rho_S(T)X_S(T)\frac{\partial T}{\partial t} \\
 & + L\rho_L(T)X_L(T)\left(\frac{\partial T}{\partial t} + VT\right) \\
 & - q\rho_S(T)\frac{\partial S}{\partial t} = \text{div}(\lambda(T)T)
 \end{aligned}
 \tag{Eqn. 5}$$

where X_S is specific heat of the solid phase, X_L is the specific heat of the liquid phase, λ is heat conduction coefficient of alloy and depends on temperature and q is crystallization heat of alloy.

The heat conduction equation for mold (subscript k indicates mold material) takes the form:

$$\rho_k(T)X_k(T)\frac{\partial T}{\partial t} = \text{div}(\lambda_k(T)T).
 \tag{Eqn. 6}$$

Material Characteristics

In this paper, for the process simulation modeling, commercial A356 aluminum cast alloy is used in simulations. The chemical composition of the alloy is given in Table 1.

In general, the liquid fraction used in semi-solid processes typically ranges from 50 to 70%.²⁶ Dependence of the liquid fraction and temperature is shown in Figure 1. Based

Table 1. Chemical Composition of Aluminum Alloy A356

Elements	Al	Si	Mg	Fe	Ti
wt%	92.667	6.9	0.34	0.08	0.013

on the material's database in the commercial software, A356 alloy is slurry with 50% of the liquid phase at approximately 581 °C. Also, A356 alloy is slurry with 70% of the liquid phase at a temperature of 606 °C. Solidus and liquidus temperatures are 521 and 623 °C, respectively.

1.1 Description of a Three-Dimensional Model

The 3D model of the casting is an important input for design and analysis. In this paper, solid modeling of electronic part cover is conducted by means of CATIA V5, as shown in Figure 2.

In order to achieve filling with the same distance from shot to each casting cavity, the biscuit is set in the center of casting. Figure 3 shows the comparison between mold design in the conventional die casting and semi-solid metal die casting. SSM filling behavior causes incomplete filling of the cavity when using conventional mold casting design, as shown in Figure 3a. In the conventional die casting,

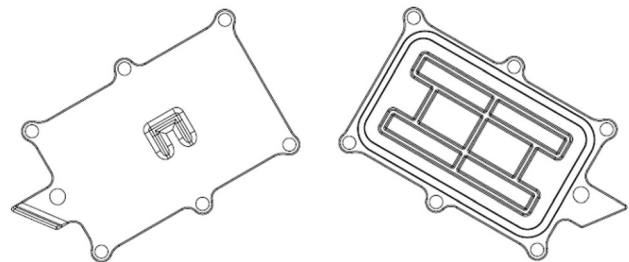


Figure 2. Cover of the electronic part.

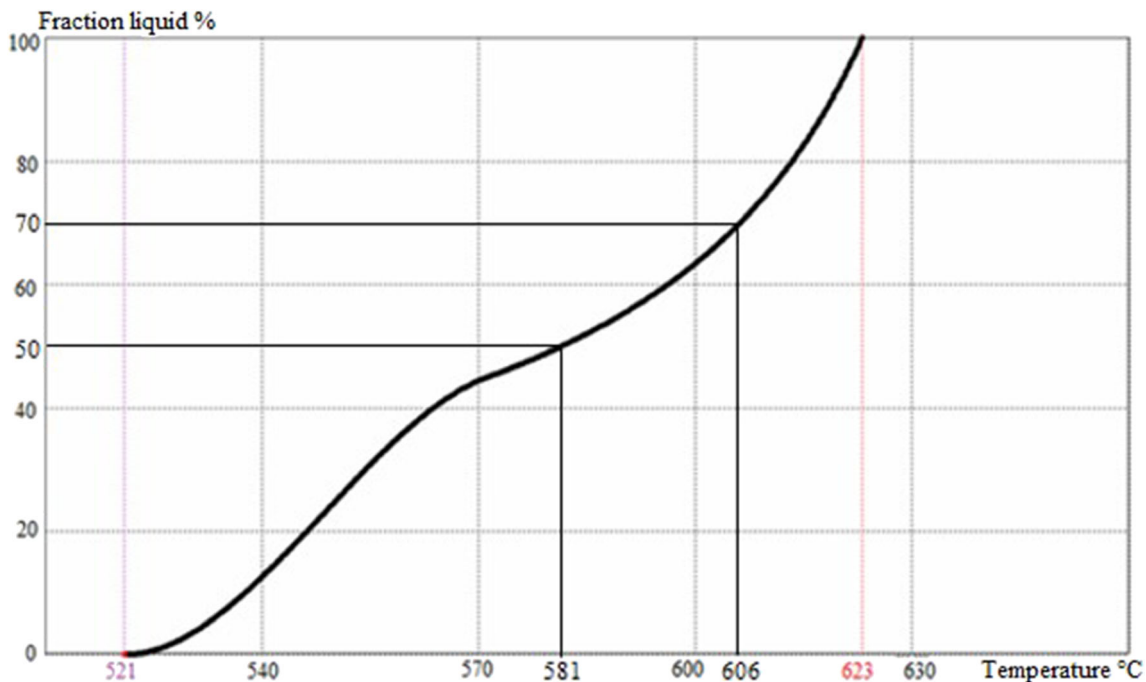


Figure 1. Liquid fraction distribution for different temperatures for A356 alloy²⁵.

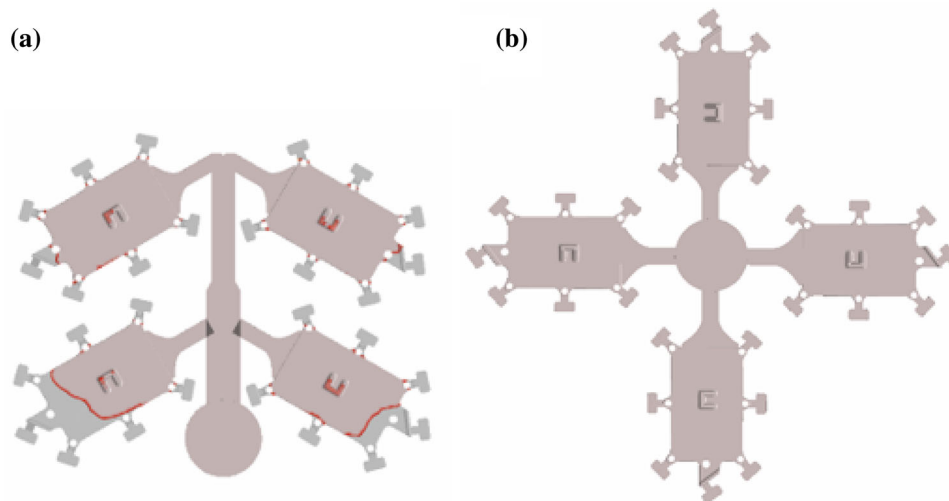


Figure 3. Layout comparison between (a) conventional high-pressure die casting and (b) semi-solid HPDC.

mold filling is very fast while the semi-solid metals flow smoothly in the mold cavity. Runners, gates and overflows were also modeled taking into account the fact that semi-solid metal slurry has a high viscosity.

In this work, the importance is given for the parameter design stage. The basic steps are presented in the next section.

Methodology

Steps for production and optimization are summarized as follows:

- (a) Selection of the significant semi-solid casting parameters having an influence on the total casting time, shrinkage and bubble formation
- (b) Selection of the appropriate design of experiments according to the number of controllable parameters and the number of levels for the controllable parameters
- (c) 3D solid modeling of the model casting
- (d) Simulations of the semi-solid HPDC process governed by the chosen design of the experiments
- (e) Data acquisition and data analysis.

Controllable Parameters

As noted earlier, casting geometry, heat parameters and velocities parameters have an influence on the formation of different phenomena during semi-solid die casting. Therefore, in this study, the liquid fraction of slurry, plunger velocity at 2nd phase and mold geometry are considered as controllable variables. Due to the high viscosity and low casting temperatures of the semi-solid slurry, there was not much space for varying some other

Table 2. Experimental Factors and Their Levels

Controllable parameters	Level 1	Level 2	Level 3
Liquid fraction [%]	50	60	70
2nd phase velocity [m/s]	1	3	5
Mold geometry	1	2	3

important design and manufacturing parameters. For example, unfilled phenomena occurred when setting the temperature of mold below 250 °C. The reason for premature solidification before complete filling of the mold is too large temperature drop during filling when mold temperatures are below 250° C. Also, the diameter of the plunger is set to be constant in order to achieve full-field casting. All of the controllable factors have three levels as shown in Table 2.

As previously mentioned, the liquid fraction of slurry is determined according to Figure 1. According to literature study for semi-solid processes, 2nd phase velocity should be less than 5 m/s.^{24,25} Hence, 2nd phase velocity has three levels as shown in Table 2. Different mold geometries are determined with the angle between the vertical plane and cavity, measured in xz plane. Mentioned angles are 0°, 30°, and 60°, presented in Figure 4. These different configurations are used as controllable parameter due to physical characteristics of semi-solid metal flow.

Design of Experiments: Taguchi Design

The literature review indicates that the Taguchi method is suitable in experimental design for designing and producing high-quality products at subsequently low cost. There are two items that should be considered before selecting a

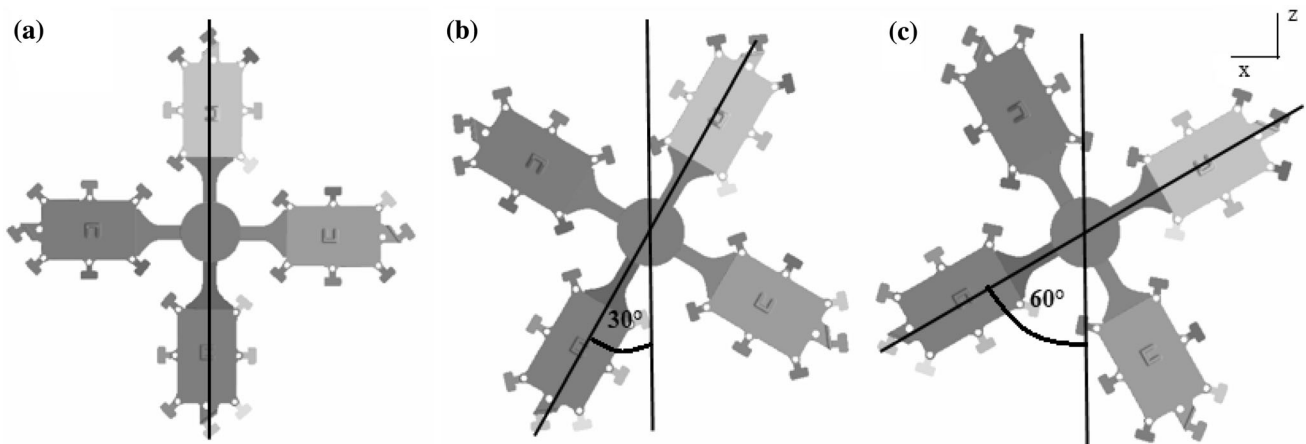


Figure 4. Different configurations: (a) mold geometry 1, (b) mold geometry 2, (c) mold geometry 3.

Table 3. Design of Experiments Based on L9 Orthogonal Array

Runs	Liquid fraction [%]	2nd phase velocity [m/s]	Mold geometry (configuration)
1	50	1	1
2	50	3	2
3	50	5	3
4	60	1	2
5	60	3	3
6	60	5	1
7	70	1	3
8	70	3	1
9	70	5	2

particular Taguchi's orthogonal array: (1) the number of controllable parameters and (2) the number of levels for the controllable parameters. Therefore, Taguchi's L9 orthogonal array is selected for three controllable variables with three levels in order to organize the experimental design. Design of experiments is given in Table 3.

In the computer simulation, it is possible to predict air entrapment and identify the location and shape of porosity. Thus, the quality characteristic is the porosity level expressed through shrinkage and bubble formation. Lower cycle time enables faster or mass production. Consequently, the third observed casting parameter is the total casting time. It is important to emphasize that the unit of measurement for bubble formation is a percentage, and it stands for maximal bubble formation in the specific area. Also, total casting time stands for the time required until the alloy reaches a temperature of 300 °C.

In this study, grey relational analysis is adopted to find optimal controllable variables for multi-objective function. As mentioned earlier, three quality objectives of the

process were chosen, including the total casting time, shrinkage of the material and bubble formation. Desirable for the casting processes are the small values of the total casting time, shrinkage of material and bubble formation. Furthermore, the optimal combination of the process parameters was found. Also, to find the influence of the controllable process factors on the multi-objective function, a statistical analysis of variance is performed. These terms are explained in more detail below.

Simulation Setup

After selection of the controllable parameters and appropriate design of experiments, it is necessary to perform 3D solid modeling. Then, the 3D casting model is imported into the commercial software as the *stp* file. The total number of cells was around 2,020,050, and dimension of the cell was 1.648 mm. The initial temperature of H13 mold was set to 250 °C, and the injection pressure at the 2nd phase was set to 100 MPa. The chosen design of experiments dictates the other casting process parameters and the design.

The final results are also influenced by heat transfer (thermal boundary conditions) across the interface of the hot casting (alloy) and cooler mold. A big difference in the temperature of two bodies causes the resistance of the flow of heat. Heat transfer coefficient is often used to deal with interfacial heat transfer. In this paper, the temperature dependence of the heat transfer coefficients is taken from the software's database. Initial and boundary conditions used in the simulations are summarized in Table 4.

Figure 5a, b shows liquid phase and bubble formation, respectively. It can be concluded that casting parameters and construction are properly designed.

Finished simulations are followed by collection and analysis of the data. The last step is making decisions regarding the optimal setting of control parameters.

Results and Discussion

Experimental runs of the process simulation with results are given in Table 5. Three process variables are read from

Table 4. Initial and Boundary Conditions

Liquid fraction [%]	50–70
2nd phase velocity [m/s]	1–5
Mold temperature [°C]	250
Heat transfer coefficients [kW/m ² /°C]	0.1 (300 °C)
	0.2 (400 °C)
	0.3 (450 °C)
	1 (565 °C)
	7 (590 °C)
	8.5 (600 °C)
	10 (620 °C)
	2 020 050

the report obtained after each simulation. It can be noticed that shrinkage has the maximal value in the 9th trial where the values of the liquid fraction and 2nd phase velocity are the highest. For better understating, shrinkage results of 5th run and 9th run are presented in Figure 6. Generally, it is impossible to eliminate shrinkage, but with optimization, it is possible to reduce its values. Also, it can be observed that bubble formation has minimal value during the 1st trial. Basically, bubble formation increases with the increase in the liquid fraction and with the increase in the 2nd phase velocity due to less laminar filling. The low 2nd phase velocity is essential for achieving a smooth mold filling.

From Figure 7, it can be observed that the total casting time increases with the increase in the liquid fraction. This is because, at lower liquid fractions, solidification is faster. Also, it can be seen that mold geometry 2 indicates the smallest casting times for all liquid fractions probably due to melt rheology and heat and mass transfers.

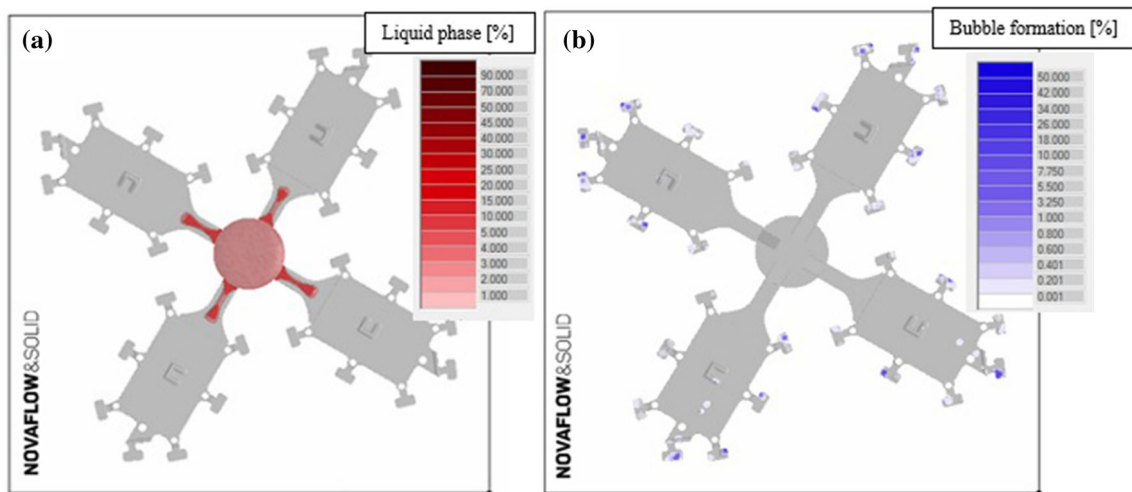


Figure 5. Simulation of (a) mold filling and (b) bubble formation.

Table 5. Total Casting Time, Shrinkage and Bubble Formation Obtained from Simulation Report

Runs	Liquid fraction [%]	2nd phase velocity [m/s]	Mold geometry	Total casting time [s]	Shrinkage [%]	Bubble formation [%]
1	50	1	1	7.7	3.911	1.05
2	50	3	2	5.6	3.928	1.11
3	50	5	3	6.25	3.926	3.25
4	60	1	2	5.937	3.959	3.58
5	60	3	3	6.585	3.903	7.59
6	60	5	1	8.1	3.939	33.81
7	70	1	3	7.076	3.923	11.04
8	70	3	1	8.682	3.957	23.47
9	70	5	2	6.303	4.004	13.67

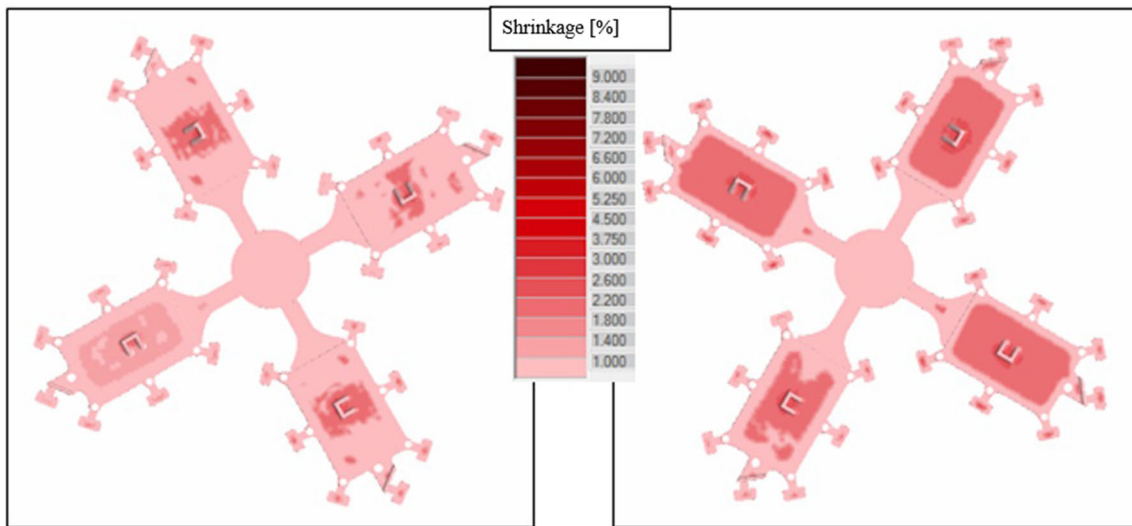


Figure 6. Comparison of simulation shrinkage results for 5th trial (left side) and 9th trial (right side).

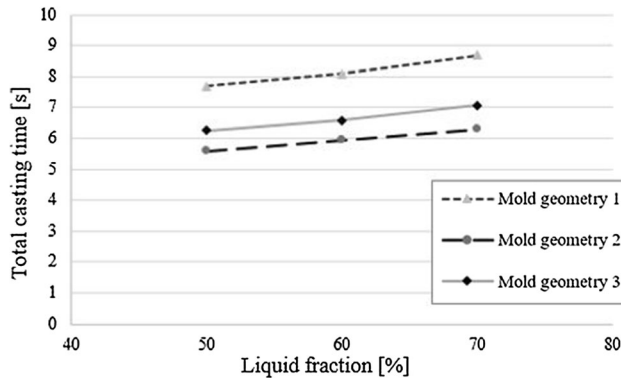


Figure 7. Influence of liquid fraction on total casting times.

Table 6. Normalized Experimental Results

Runs	Total casting time [s]	Shrinkage [%]	Bubble formation [%]
1	0.3186	0.9233	1
2	1	0.7525	0.9980
3	0.7891	0.7772	0.9328
4	0.8907	0.4480	0.9228
5	0.6804	1	0.8002
6	0.1888	0.6460	0
7	0.5211	0.8044	0.6950
8	0	0.4703	0.3157
9	0.7719	0	0.6147

Grey Relation Analysis

In this work, grey relational analysis, GRA, is used for solving complex interconnections between specific performance properties. Consequently, a grey system is used for the optimization of multiple performance characteristics. Through this analysis, this complex multiple response optimization problem is simplified into the optimization of a grey relational grade, GRG. The procedure for determining GRG is discussed below.

The first step of the GRA is the grey relation generation performed in order to transfer the original array to a comparable array. During this step, the total casting time, shrinkage of the material and bubble formation are normalized between zero and one.

Depending on the characteristics of a data array, various methodologies of normalizing value of the original array are available. In this study, the normalized value of the original array for the total casting time, shrinkage of the

material and bubble formation is the lower the better and can be expressed as:

$$x_{ij} = \frac{\max y_{ij} - y_{ij}}{\max y_{ij} - \min y_{ij}} \quad \text{Eqn. 7}$$

where x_{ij} is the value after the grey relation generation, $\min y_{ij}$ is the smallest value of original data y_{ij} and $\max y_{ij}$ is the largest value of y_{ij} . Subscript j stands for response and i for experiment or simulation.

Table 6 shows the normalized values of total casting time, shrinkage of the material and bubble formation.

A determination of the reference array x_{0j} is the next step. The performance of simulation i is considered as the referent for the response j if the value after the grey relation generation x_{ij} is equal to one or nearer to one than the value for any other simulation.

In the third step of the GRA, the grey relation coefficient, ζ_{ij} , is used for determining how close x_{ij} and x_{0j} are. The grey relation coefficient ζ_{ij} can be determined as:

$$\zeta_{ij} = \frac{\Delta_{\min} + \zeta \Delta_{\max}}{\Delta_{ij} + \zeta \Delta_{\max}} \quad \text{Eqn. 8}$$

where $\zeta \in (0, 1]$ is the index of distinguishability called distinguishing coefficient. In this study, the value of coefficient ζ is assumed as 0.5. Although different distinguishing coefficients may lead to different solution results,²⁷ it is generally set at 0.5 to allocate equal weights to every parameter.²⁸ It can be seen from the above equation when x_{ij} and x_{0j} are closer, the grey relation coefficient is the larger.

$$\Delta_{ij} = |x_{0j} - x_{ij}| \quad \text{Eqn. 9}$$

$$\Delta_{\min} = \min\{\Delta_{ij}, i = 1, 2, \dots, m; j = 1, 2, \dots, n\}, \quad \text{Eqn. 10}$$

$$\Delta_{\max} = \max\{\Delta_{ij}, i = 1, 2, \dots, m; j = 1, 2, \dots, n\}. \quad \text{Eqn. 11}$$

The last step is the determination of the grey relation grade, GRG, which presents the measurement formula for quantification in grey relational space. It is calculated using the equation:

$$y_i = \frac{1}{n} \sum_{j=1}^n \zeta_{ij} \quad \text{Eqn. 12}$$

where n is a number of process response.

The grey relational grade signifies the degree of similarity between the comparability array and the reference array. Therefore, the best choice would be the experiment or simulation with the highest grey relation grade. Table 7 shows the grey relation coefficients and grade for each experiment where the highest grey relational grade is the order of 1.

For better understanding difference in results between the experiment with the lowest grey relational grade (run 9)

Table 7. Grey Relational Coefficients and Grey Relational Grade

Runs	Total casting time [s]	Shrinkage [%]	Bubble formation [%]	Grade	Grey order
1	0.4232	0.8669	1	0.7634	3
2	1	0.6689	0.9960	0.8883	1
3	0.7033	0.6918	0.8815	0.7589	4
4	0.8205	0.4753	0.8662	0.7207	5
5	0.6100	1	0.7145	0.7748	2
6	0.3813	0.5855	0.3333	0.4334	8
7	0.5108	0.7189	0.6212	0.6169	6
8	0.3333	0.4856	0.4222	0.4137	9
9	0.6867	0.3333	0.5648	0.5283	7

and the experiment with the highest grey relational grade (run 2), bubble formation results are presented in Figure 8. Overflows are applied for avoiding air entrapments in the casting. However, the filling simulation revealed two critical areas, detail A and detail B in Figure 8a. These regions have a high risk of defects. A significant reduction in air entrapments is shown in Figure 8b.

The nearest optimal controllable parameter combination is in experiment 2. Table 8 shows the means of the grey relation grades for each level of controllable parameters. For example, means of the grey relation grades for level 1 of die geometry is calculated by summing grades of 1st, 6th and 8th experiments (according to Table 3) and dividing calculated sum by three. The optimal levels, levels with the highest grey relation grade, of the process parameters are low liquid fraction (50%), low plunger velocity at 2nd phase (1 m/min) and the angle of 60° between the vertical plane and cavity, measured in xz plane. These optimal levels are shown in bold in Table 8.

The optimal process parameters can reduce the risk of the shrinkage and enhance the stability of the process.

Analysis of Variance

A method used in this study for finding out the importance of the controllable parameter on the performance characteristic is called the analysis of variance, ANOVA. This is accomplished calculating the percentage contribution by the sum of squares of each of the process parameters to the total sum of squared deviations. SS stands for the sum of squared deviations for a considered factor and is calculated using the equation:

$$SS = \frac{k}{m} \sum_{t=1}^k y_t^2 - \frac{y^2}{m} \quad \text{Eqn. 13}$$

where k is the number of levels, y_t is the total sum of the grey relation grade at t th level, y is the total sum of the grey relation grade and m is the total number of experiments.

SS_T stands for the total sum of the squared deviations and can be determined as:

$$SS_T = \sum_{i=1}^m \sum_{j=1}^n y_{ij}^2 - \frac{y^2}{m} \quad \text{Eqn. 14}$$

where y_{ij} are individual observations.

As mentioned, the percentage contribution P is calculated using the equation:

$$P = \frac{SS}{SS_T} \quad \text{Eqn. 15}$$

The main purpose of higher viscosity and density of semi-solid slurry is to reduce the porosity and to achieve a better

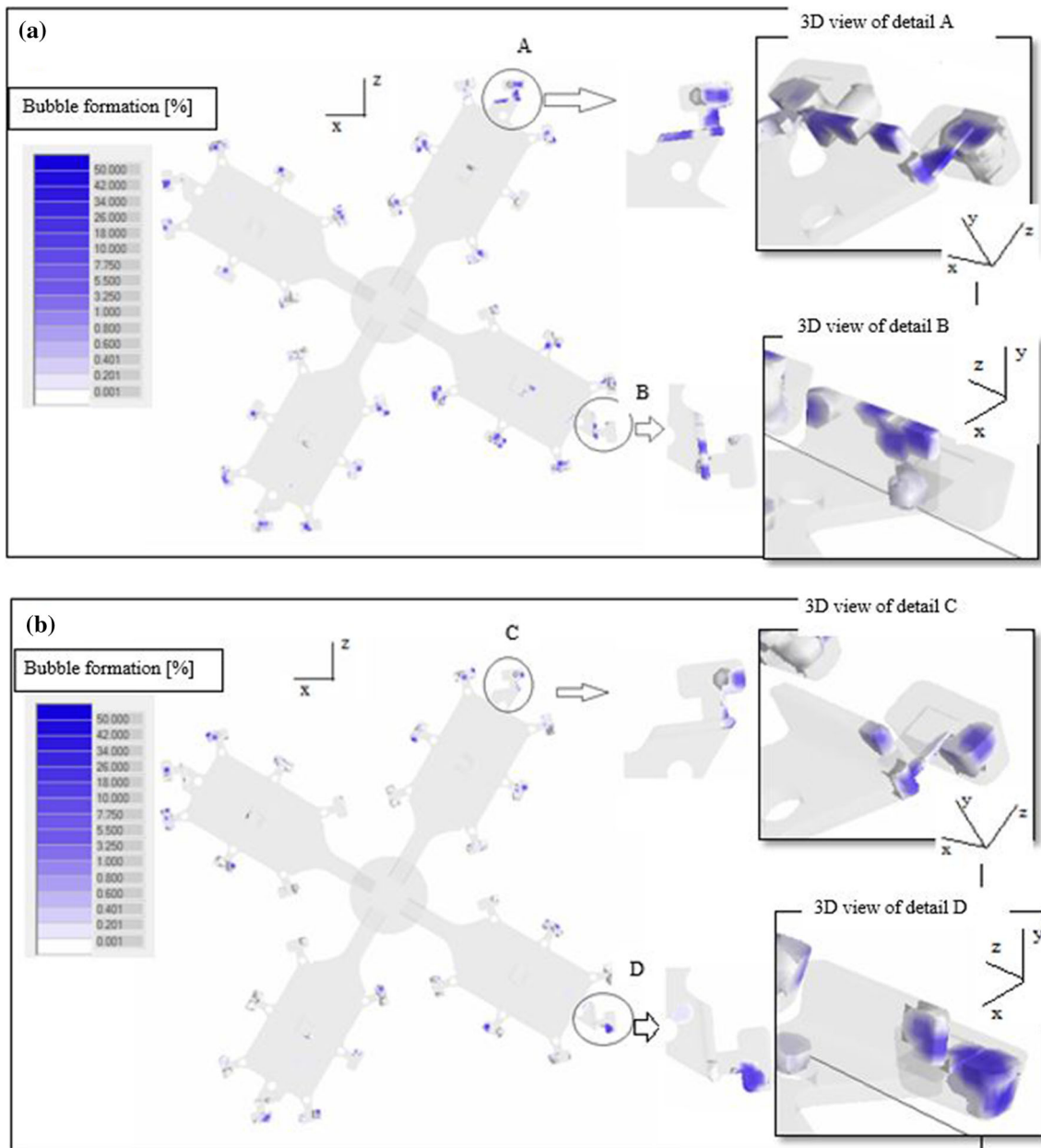


Figure 8. Comparison of bubble formation results between (a) run with the worst grey relational grade (run 8) and (b) run with the best grey relational grade (run 2).

Table 8. Response Table for Grey Relational Grade

Parameter	Level 1	Level 2	Level 3	Rank (max-min)
Liquid fraction [%]	0.8035	0.6430	0.5196	1 (0.2839)
2nd phase velocity [m/s]	0.7003	0.6923	0.5735	3 (0.1268)
Mold geometry	0.5368	0.7124	0.7169	2 (0.1801)

Table 9. Percentage Contribution of Input Parameters on Response Variables

	SS	Percentage contribution [%]
Liquid fraction [%]	0.1216	55
2nd phase velocity [m/s]	0.0302	14
Mold geometry	0.0334	15
SS _T	0.2205	

casting surface. That is why liquid fraction influenced the grey relation grade the most, as shown in Table 9.

Conclusion

To provide high-quality casting, the semi-solid HPDC process of A356 aluminum alloy is analyzed. Considering viscosity of semi-solid slurry and the fact that semi-solid metals flow smoothly in the mold cavity, the biscuit is set in the center of the cavity. On the other hand, porosity and shrinkage are main failures that decrease efficiency; therefore, to prevent microporosity and to reduce cycle time, optimal controllable parameters were investigated. Taguchi's L9 orthogonal array is used for process design, and the computer simulation technology is utilized to optimize processes parameters and design. The grey relational analysis shows that the best performance characteristics were obtained with the liquid fraction of 50%, plunger velocity at 2nd phase of 1 m/min and the angle of 60° between the vertical plane and cavity, measured in *xz* plane.

Author contributions ID contributed to the study conception and design. Solid modeling in CATIA V5 was performed by SJ and ID. JK designed Taguchi plan of the experiments. SJ and ID performed the simulations. The Taguchi-based grey relational analysis was performed by DB and JK. The first draft of the manuscript was written by ID. All authors peer-reviewed paper writing and editing. All authors reviewed the final manuscript.

Funding

This research received no external funding.

Compliance with Ethical Standards

Conflict of interest The authors declare no conflict of interest.

REFERENCES

1. D.B. Spencer, R. Mehrabian, M.C. Flemings, Rheological behavior of Sn–15%Pb in the crystallization range. *Metall. Mater. Trans. B* **3**(7), 1925–1932 (1972)
2. R. Koeune, J.P. Ponthot, in *Advanced Computational Materials Modeling: From Classical to Multi-scale Techniques*, ed. by M.V. Júnior, E.A. de Souza Neto, P.A. Munoz-Rojas (Wiley, Berlin, 2011), p. 205. <https://doi.org/10.1002/9783527632312.ch6>
3. A. Pola, M. Tocci, P. Kapranos, Microstructure and properties of semi-solid aluminum alloys: a literature review. *Metals* **8**(3), 181 (2018)
4. A. Fabrizi, S. Capuzzi, A. De Mori, G. Timelli, Effect of T6 heat treatment on the microstructure and hardness of secondary AlSi9Cu3(Fe) alloys produced by semi-solid SEED process. *Metals* **8**(10), 750 (2018)
5. J. Wang, A.B. Phillion, G. Lu, Development of a visco-plastic constitutive modeling for thixoforming of AA6061 in semi-solid state. *J. Alloys Compd.* **609**, 290–295 (2014)
6. M.S. Salleh, M.Z. Omar, J. Syarif, M.N. Mohammed, An overview of semisolid processing of aluminium alloys. *ISRN Mater. Sci.* (2013). <https://doi.org/10.1155/2013/679820>
7. Q.Y. Pan, M. Arsenault, D. Apelian, M.M. Makhlof, SSM processing of A1B 2 grain refined Al–Si alloys, in *Transactions of the American Foundry Society*, pp. 273–287 (2004). ISBN: 0-87433-277-X
8. B. Zhou, Y. Kang, M. Qi, H. Zhang, G. Zhu, R-HPDC process with forced convection mixing device for automotive part of A380 aluminum alloy. *Materials* **7**(4), 3084–3105 (2014)
9. X. Jian, T.T. Meek, Q. Han, Refinement of eutectic silicon phase of aluminium A356 alloy using high-intensity ultrasonic vibration. *Scr. Mater.* **54**(5), 893–896 (2006)
10. B.G.E., M. Nouri, R. Beygi, M.Z. Mehrizi, A. Nouri, M. Ebrahimi, Effects of Sr on the microstructure of electromagnetically stirred semi solid hypoeutectic Al–Si alloys, in *6th International Symposium on Metalcasting, Shape Casting*, pp. 133–140 (2016). https://doi.org/10.1007/978-3-319-48166-1_17S
11. S. Nafisi, R. Ghomashchi, *Semi-Solid Processing of Aluminum Alloys* (Springer, Basel, 2016), pp. 30–33. ISBN 978-3-319-40335-9
12. O. Bustos, S. Ordoñez, R. Colás, Rheological and microstructural study of A356 alloy solidified under magnetic stirring. *Int. Metalcast.* **7**(1), 29–37 (2013). <https://doi.org/10.1007/BF03355542>
13. V.M. Nimbalkar, B. Bhanushali, M. Mohape, S.G. Pandav, V.P. Deshmukh, S. Dineshraj, S.C. Sharma, Development of thin walled A-356 components by new rheocasting semi-solid metal processing technology (NRC). *Mater. Sci. Forum* **830**, 27–29 (2015)
14. F. Czerwinski, *Magnesium Injection Molding* (Springer, New York, 2008), pp. 135–145. ISBN 978-0-387-72528-4
15. J.L. Fu, H.J. Jiang, K.K. Wang, Influence of processing parameters on microstructural evolution and tensile properties for 7075 Al alloy prepared by an ECAP-based SIMA process. *Chin Shu Hsueh Pao* **31**(4), 337–350 (2018). <https://doi.org/10.1007/s40195-017-0672-6>
16. A. Leatham, A. Ogilvy, P. Chesney, J.V. Wood, Osprey process-production flexibility in materials manufacture. *Met. Mater.* **5**(3), 140–143 (1989)
17. A. Heinz, A. Haszler, C. Keidel, S. Moldenhau, R. Benedictus, W.S. Miller, Recent development in aluminium alloys for aerospace applications. *Mater. Sci. Eng. A* **280**(1), 102–107 (2000)
18. W.S. Miller, L. Zhuang, J. Bottema, A. Wittebrood, P. De Smet, A. Haszler, A. Vieregge, Recent

- development in aluminium alloys for the automotive industry. *Mater. Sci. Eng. A* **280**(1), 37–49 (2000)
19. M. Sadeghi, J. Mahmoudi, Experimental and theoretical studies on the effect of die temperature on the quality of the products in high-pressure die-casting process. *Adv. Mater. Sci. Eng.* **2012**, 434605 (2012)
 20. G.O. Verran, R.P.K. Mendes, M.A. Rossi, Influence of injection parameters on defects formation in die casting Al12Si1, 3Cu alloy: Experimental results and numeric simulation. *J. Mater. Process. Technol.* **179**(1–3), 190–195 (2006)
 21. M. Avalor, G. Belingardi, M.P. Cavatorta, R. Doglione, Casting defects and fatigue strength of a die cast aluminium alloy: a comparison between standard specimens and production components. *Int. J. Fatigue* **24**(1), 1–9 (2002)
 22. S. Nourouzi, H. Baseri, A. Kolahtooz, S.M. Ghavamodini, Optimization of semi-solid metal processing of A356 aluminum alloy. *J. Mech. Sci. Technol.* **27**(12), 3869–3874 (2013)
 23. H. Khosravi, R. Eslami-Farsani, M. Askari-Paykani, Modeling and optimization of cooling slope process parameters for semi-solid casting of A356 Al alloy. *Trans. Nonferr. Met. Soc. China* **24**(4), 961–968 (2014)
 24. Y.B. Suslu, M.S. Acar, M. Senol, M. Mutlu, O. Keles, Optimization in novel partial-solid high pressure aluminum die casting by Taguchi method, in *TMS Annual Meeting & Exhibition*, pp. 293–300 (2018). https://doi.org/10.1007/978-3-319-72284-9_40
 25. NOVAFLOW&SOLID 6.4; Manual—2018-08-29; NovaCastSystems AB
 26. P.K. Seo, M.D. Lim, C.G. Kang, Numerical visualization of viscosity in phase transformation forming process with controlled liquid fraction. *J. Mater. Process. Technol.* **153**, 450–456 (2004)
 27. R. Rao Venkata, *Advanced Modeling and Optimization of Manufacturing Processes: International Research and Development* (Springer, London, 2010), pp. 10–13. ISBN 978-0-85729-014-4
 28. P. Achuthamenon Sylajakumari, R. Ramakrishnasamy, G. Palaniappan, Taguchi grey relational analysis for multi-response optimization of wear in co-continuous composite. *Materials* **11**(9), 1743 (2018). <https://doi.org/10.3390/ma11091743>

Publisher's Note Springer Nature remains neutral with regard to jurisdictional claims in published maps and institutional affiliations.